Conformational Effects and Configurational Splitting in ^{13}C NMR Spectra of Synthetic Polymers As Investigated by *ab Initio* Individual Gauges for Localized Molecular Orbitals (IGLO) Calculations

R. Born and H. W. Spiess*

Max-Planck-Institut für Polymerforschung, Postfach 3148, D-55021 Mainz, Germany

Received July 10, 1995; Revised Manuscript Received September 5, 1995[⊗]

ABSTRACT: The inhomogeneous broadening of solid state ^{13}C spectra of glassy polymers and the configurational splitting observed in solution spectra are analyzed by a unifying approach. The method combines conformational statistics and *ab initio* IGLO calculations to obtain simulated solid state and solution spectra. A number of polymers of different structural classes are investigated, including poly(ethylene), atactic poly(propylene), poly(vinyl chloride), and poly(methyl methacrylate). For most systems a remarkable degree of agreement between simulation and experiment is achieved for both the solid state NMR and the configurational splitting. Furthermore, the influence of geometric parameters on the chemical shift, the validity of the *γ-gauche* effect, an MO analysis, and the role of the anisotropic part of the chemical shift tensor as a source of structural information are considered.

1. Introduction

A characteristic feature of most synthetic polymers is the considerable flexibility of the chains. In solution or in the amorphous solid state the dihedral angles along the main chain are not restricted to well-defined values, but are subject to a statistical probability distribution. This probability distribution depends on the molecular details of the polymer in question. Its theoretical evaluation and experimental characterization is essential for the understanding of polymers in noncrystalline phases such as solutions or the glassy amorphous state.

Nuclear magnetic resonance (NMR) is sensitive not only to the constitution of a molecule but also to its local geometry. The influence of the conformational environment on NMR spectra has long been known under the name of the *γ-gauche* effect (*vide infra*): The shielding experienced by a carbon atom with γ-neighbors in a *trans*-position differs from a carbon with *gauche*-positioned γ-neighbors. NMR as a local method is insensitive to long range order and might thus be useful for the investigation of the local structure of disordered systems.

In solution, the polymers undergo rapid conformational transitions and only averaged resonance lines are observed. As both the conformational statistics and the exact geometry depend on the stereostatistics, *i.e.* configuration, a typical ^{13}CNMR spectrum of an atactic vinyl polymer in solution consists of numerous relatively sharp lines, that can be assigned to the various sequences of *meso* (*m*) and *racemic* (*r*) diads. Thus one observes a **configurational** splitting. In fortunate cases even heptad compositions can be distinguished. In the last two decades, an empirical method based on a simplified parametrization of the *γ-gauche* effect has been devised that allows the quantitative interpretation of numerous vinyl polymer spectra,[1] (see however the failure of the method in the special case of poly(methyl methacrylate) (PMMA)[2]).

In the glassy amorphous state, the conformational disorder is frozen on the NMR time scale. Thus we do not find averaged spectra but inhomogeneously broadened resonance lines in ^{13}C Cross Polarization/Magic Angle Spinning (CP/MAS) spectra. Within the resonance lines every frequency (=every chemical shift) corresponds to a certain geometry. The distribution of chemical shifts reflects the distribution of geometries which in turn is governed mainly by the conformational statistics in the glassy state; the observed spread in resonance lines is thus of **conformational** origin. Although this qualitative interpretation of experimental solid state NMR spectra is quite clear, a quantitative explanation has been missing until recently.[3]

To obtain a sound theoretical and quantitative understanding of these two aspects of the NMR of polymers, *viz.* **configurational** splitting and **conformational** broadening, we employ modern *ab initio* quantum chemistry methods (**I**ndividual **G**auges for **L**ocalized Molecular **O**rbitals, IGLO[4–6]) together with theoretical models of the conformational statistics (**R**otational **I**someric **S**tate (RIS) models in the spirit of ref 7). As a first example, the investigation of the solid state spectrum of poly(isobutylene) (PIB) has already been published.[3] A more detailed account focusing on methodical and technical aspects is in preparation.[8] In this paper, we concentrate on principles and results rather than technique. Our objective is 2-fold: First, we want to demonstrate the essentials of the method (section 2) on a simple example, atactic poly(propylene) (aPP), and the wealth of results that can be obtained by the combination of statistical mechanics, quantum chemistry, and NMR (section 3). Secondly, we investigate various polymer systems covering different structural classes (Table 1, Figure 1), including polyolefins with one or two side groups, unsaturated systems, and a system with an extended side group, to show the realm of applicability of the method by presenting some selected results (section 4). A special section is devoted to the results on configurational splitting (section 5), which is mostly self-contained for the convenience of the reader interested only in this aspect.

2. Method

Atactic Poly(propylene). To avoid a clumsy general notation, we will refer to the concrete example of

* To whom correspondence should be addressed.

[⊗] Abstract published in *Advance ACS Abstracts,* October 15, 1995.

0024-9297/95/2228-7785$09.00/0

Table 1. List of Investigated Polymers[a]

polymer	abbrev	characteristic feature	statistical model (ref)
poly(ethylene)	PE	simplest polymer	9
atactic poly(propylene)	aPP	polyolefin, one side group	10
poly(isobutylene)	PIB	polyolefin, two side groups	11
1,4-poly(butadiene)	PBD	unsaturated	12
1,4-poly(isoprene)	PIP	unsaturated, side group	13
poly(vinyl chloride)	PVC	contains heteroatom	14–16
poly(methyl methacrylate)	PMMA	extended side group	17

[a] The characteristic features of the system and the statistical model employed are also included. The corresponding model molecules are depicted in Figure 1.

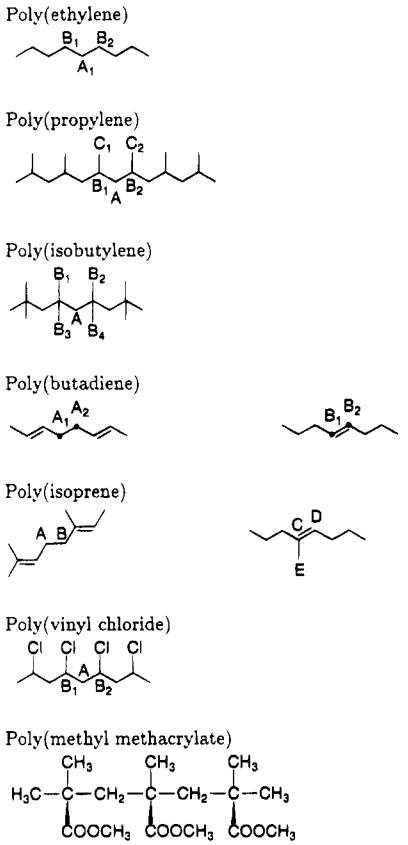

Figure 1. Model molecules for the investigated polymer systems. For PBD and PIP, two different segments have been investigated to reduce the computation time.

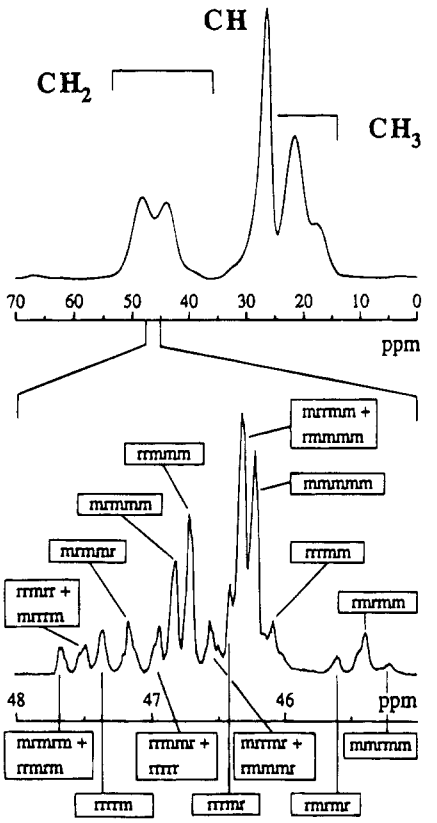

Figure 2. ^{13}CCP/MAS spectrum of aPP (top) shows broad structured resonances, especially in the methylene and methyl regions. The spread in the solution spectrum of the methylene region (bottom) is much smaller; the numerous sharp lines belong to different configurations. Reprinted with small changes from ref 19.

atactic poly(propylene) (aPP) in this section. For the sample chosen, we have almost perfect Bernoullian configurational statistics with equal probability for m and r diads, $p_m = p_r = 0.5$ (within experimental error, the configurational distribution of ideally atactic poly(propylene) is met, $(mm) = 25\%$, $(mr) = 50\%$, $(rr) = 25\%$[18]). The calorimetric glass transition temperature is ≈270 K. Both the solid state CP/MAS spectrum of the polymer glass and the solution spectrum are shown in Figure 2 (reprinted for reader convenience from ref 19). Conformational broadening and configurational splitting are clearly visible. In the solid state spectrum, the methylene resonance is richly structured, displaying two main contributions and a high-field shoulder. The methyl peak is structured, too, whereas the methine resonance is comparatively narrow. The high spinning speed precludes any broadening due to residual chemical shift anisotropy. Motional broadening can be excluded below the glass transition temperature, too.[19] In the solution spectrum of the methylene region numerous peaks occur which reflect configurational splitting due to different hexad compositions.

Conformational and Configurational Statistics. The geometry of the central part of a poly(propylene) chain depends on the configuration (diad character m/r) *and* the conformation (dihedral angles ϑ_i). Both, configuration and conformation, are subject to a statistical probability distribution function. For simplicity, we refer to the model molecule for quantum chemistry calculations, a hexamer with CH_3 as the end groups (Figure 3). We will concentrate on the central part of the molecule and neglect the influence of remote parts and less important geometry parameters. Then, the combined probability distribution function for configuration and conformation depends on three discrete parameters, the relative chiralities of the three central diads ($x_i = m, r$; $i = 1-3$) and four continuous variables, the relevant dihedral angles ($\vartheta_j \in [0°, 360°]$; $j = 1, ..., 4$). This zone of interest and well-defined geometry within an extended polymer chain is not arbitrary. Only with the dihedral angles $\vartheta_1, ..., \vartheta_4$ and the configuration $x_1, ..., x_3$ given is the geometrical position of the γ-neighbors of the central methylene unit (A) and the two neighboring methyl carbons (C_1, C_2) (see Figures 1 and 3) precisely defined. As we know about the relevance of the *γ-gauche* effect for the chemical shift, this

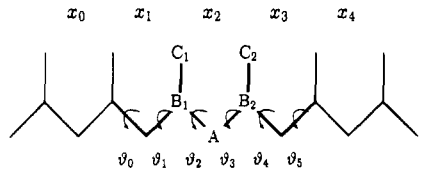

Figure 3. Model molecule for poly(propylene), a hexamer with methyl end groups and many degrees of freedom. The γ-neighbors of the central methylene (A) and methyl (C_1, C_2) units are fixed by defining the central diads x_1, x_2, x_3 and the dihedral angles ϑ_1, ϑ_2, ϑ_3, ϑ_4. These parameters have to be set to definite values; then a region of well-defined geometry within the model molecule is established; it is depicted by bold lines. For the γ-neighbors of the methine units (B_1, B_2) the additional dihedral angles ϑ_0 and ϑ_5 should be set to defined values, too. As the experimental resonance of the methine unit (Figure 2) is very narrow and of little interest, this computer time consuming refinement has been omitted.

is the minimum size of the region of well-defined geometry. In Figure 3 it is depicted in by bold lines.

On the other hand, a larger segment of well-defined geometry (*e.g.*, by including the dihedral angles ϑ_0 and ϑ_5) can be taken into account only at the price of a considerably longer computation time (*vide infra*).

The relevant probability distribution function can be split into an *a priori* configurational distribution and a conditional conformational probability function, depending only parametrically on the configuration.

$$p(x_1,x_2,x_3,\vartheta_1,\vartheta_2,\vartheta_3,\vartheta_4) = p_{\text{config}}(x_1,x_2,x_3)\, p_{\text{conform}}(\vartheta_1,\vartheta_2,\vartheta_3,\vartheta_4|x_1,x_2,x_3) \quad (1)$$

The configurational statistics p_{config} is fixed by the conditions of the chemical synthesis and does not change with temperature; it can be quite easily inferred from a quantitative ^{13}C solution spectrum. In contrast to this, the conformational probability function p_{conform} is a complicated function of the four continuous variables ϑ_i and, *via* the Boltzmann factor $\exp(-E(\vartheta_1, ..., \vartheta_4)/k_BT)$, depends on temperature. The exact functions $E(\vartheta_1,...,\vartheta_4)$ or $p_{\text{conform}}(\vartheta_1,\vartheta_2,\vartheta_3,\vartheta_4|x_1,x_2,x_3)$ are far from being known. A simplified rotational isomeric state (RIS) model assumes that the dihedral angles may adopt only a few (n) fixed values $\{\Theta_1, ..., \Theta_n\}$ which correspond to the minima of the energy curve. For poly(propylene), a model with five states (two *trans* (t) states and three *gauche* (g) states)[10] is widely accepted. Then, the probability function is more easily described as a function of discrete variables.

$$p^{\text{RIS}}_{\text{conform}}(\vartheta_1,...,\vartheta_4|x_1,x_2,x_3) \qquad \vartheta_i \in \{\Theta_1, ..., \Theta_{n=5}\}, \quad x_i \in \{m, r\} \quad (2)$$

The numerical values for a given polymer can be obtained from the respective theoretical model. The models rely on either an analysis of the energy hypersurface, a Monte Carlo (MC), or molecular dynamics (MD) simulation. Here, we must emphasize that the RIS models and probability distributions mostly refer to an isolated chain in a Θ solvent. Naturally, a polymer glass is something completely different, but it is widely believed that the isolated chain RIS models provide also a valid description for the amorphous solid state. Indeed, a series of well-known neutron scattering experiments (see, *e.g.*, ref 20) has shown that the radii of gyration in bulk do not differ much from those obtained in solution; thus the validity of the random chain model is established on a larger (>10 Å) length scale. By investigating such a model *via* NMR experiments, we can now probe the local statistics and see whether this equivalence still holds on a truly microscopic level.

IGLO Calculations of Chemical Shifts. In quantum mechanical terms, the chemical shift σ is the mixed second-order perturbation of the energy expectation value of the molecule with respect to the exterior magnetic field **B** and the nuclear magnetic moment $\boldsymbol{\mu}$ of the nucleus K in question.

$$\sigma^{\text{K}}_{\alpha\beta} = \frac{\partial^2 E}{\partial \mu^{\text{K}}_\alpha \partial B_\beta} \qquad \alpha, \beta = x, y, z \quad (3)$$

where $E = \langle \mathscr{H} \rangle$ and $\mathscr{H}$ is the full Hamiltonian of the system including the magnetic perturbations. In a numerical implementation, problems occur that are related to the approximate character of all quantum chemical calculations and the fact that the magnetic field enters the Hamiltonian only *via* its vector potential

$$\mathbf{B} = \nabla \times \mathbf{A} \quad (4)$$

which is subject to gauge transformations

$$\mathbf{A} \rightarrow \mathbf{A}' = \mathbf{A} + \nabla\lambda \quad (5)$$

Both difficulties can be avoided by the (Hartree–Fock level) IGLO scheme (**I**ndividual **G**auges for **L**ocalized Molecular **O**rbitals) which has been successfully applied to a great number of compounds and has been essential in understanding chemical shifts.[6] For further details,[5,21] as well as an account on competing methods (GIAO,[22-25] LORG[26,27]), we refer to the literature.

As can be seen from eq 3, the chemical shift is a second rank tensor. To the first order, only the symmetric part of the tensor has an influence on the spectrum. For simplicity, we denote the symmetrized tensor by $\sigma_{\alpha\beta}$ as well. In liquid NMR and specially designed solid state experiments (MAS), only the isotropic part of the tensor

$$\sigma_{\text{iso}} = \frac{1}{3}(\sigma_{xx} + \sigma_{yy} + \sigma_{zz}) \quad (6)$$

is detected. The investigation of the anisotropy of the chemical shift in solid state NMR requires special techniques (*vide infra*, section 3).

Procedure for the Simulation of Experimental Spectra. To obtain an *ab initio* simulation of the experimental spectrum of aPP, we use the most advanced statistical model for poly(propylene)[10] and calculate $p^{\text{RIS}}_{\text{conform}}(\vartheta_1,...,\vartheta_4|x_1,x_2,x_3)$ for all configurational sequences (x_1, x_2, x_3). For the most importance sequences $k^j = (x^j_1, x^j_2, x^j_3; \vartheta^j_1, \vartheta^j_2, \vartheta^j_3, \vartheta^j_4)$ with a high probability we generate Cartesian coordinates of the model molecule displayed in Figures 1 and 3 by a force field minimization with fixed x^j_1, x^j_2, x^j_3 and ϑ^j_1 ..., ϑ^j_4; the resulting geometries are denoted $G^j = G(k^j)$. For this purpose we use the widespread **C**onsistent **V**alence **F**orce **F**ield (CVFF) of the DISCOVER package.[28] CVFF is a second-order force field. Apart from the ordinary terms for the elongation of a bond (*stretch*), the bending of a bond angle (*bend*), the rotation around a σ-bond (*torsion*), and the nonbonded Coulomb and Van der Waals energies, it contains cross terms that interrelate the basic degrees of freedom. *E.g.*, two neighboring bond lengths r, r' are connected *via* $F_{rr'}(r - r_0)(r' - r'_0)$. Due to these additional terms, the force field contains numerous parameters that depend, moreover, on the chemical residues involved. Generally, the bond lengths do not differ much from one force field to

Table 2. Range of Optimized Bond Angles for Some Selected Cases[a]

polymer	central atom	observed range (deg)
aPP	CH	109–115
PIB	quaternary carbon	108–117
PE	CH_2	111–116
PMMA	quaternary carbon	102–112

[a] The geometry optimization was performed with the CVFF force field. The appreciable deviations from the tetrahedral value reflect the presence of the neighboring residues; the range is due to the influence of the adjacent dihedral angles (*cf.* Figure 10d).

another, and the torsional angles are forced to the RIS values in the present approach. Some selected results on the optimized bond angles are collected in Table 2.

These optimized geometries are then considered as representative of the geometries of the inner part of an extended polymer chain. Thus, we transfer the statistics from a long polymer chain (that is inaccessible to present day quantum chemistry calculations) to a small model molecule (that can be easily treated on a workstation).

Afterward, for each of the geometries G^j, an IGLO calculation is performed and we obtain chemical shifts for all nuclei K and all geometries G^j: $\sigma_K(G^j)$. The simulated solid state line shape is a weighted superposition of the contributions of the relevant geometries:

$$g_K(\sigma) = \sum_j p_{config}(x_1^j,x_2^j,x_3^j)\, p^{RIS}_{conform}(\vartheta_1^j,...,\vartheta_4^j|x_1^j,x_2^j,x_3^j)\, \delta(\sigma-\sigma_K(G^j)) \quad (7)$$

Note that only the nuclei K = A, B_1, B_2, C_1, C_2 in the central part of the model molecule are considered as representative of an extended polymer chain, because here the geometry is well-defined and end-group effects can be neglected. This formula shows explicitly the modular character of the method. The statistical model (ref 10 in our case), the way of generating the geometries G^j (here: CVFF empirical force field), and the quantum chemical method for the calculation of chemical shifts (here: Hartree–Fock level IGLO scheme) are building blocks that can be exchanged, if necessary. More refined statistical models, better geometries, *e.g.*, by SCF-MP (**S**elf-**C**onsistent **F**ield with **Møller–Plesset** corrections), and more sophisticated ways to obtain the chemical shift can be alike used in this formula. In contrast, the discrete nature of the sum in eq 7 with only comparatively few terms is essential in dealing with present day computing power.

To allow for deviations from the ideal RIS dihedral values, we replace the δ-function in eq 7 by a Gaussian function $s_b(x) = (1/\sqrt{2\pi}b)\exp(-x^2/2b^2)$.

$$g_K(\sigma) = \underbrace{\sum_j p_{config}(x_1^j,x_2^j,x_3^j)}_{\text{synthetic conditions}}\ \underbrace{p^{RIS}_{conform}(\vartheta_1^j,...,\vartheta_4^j|x_1^j,x_2^j,x_3^j)}_{\text{statistical model}} \times \underbrace{s_b(\sigma-\sigma_K(G^j))}_{\text{IGLO}} \quad (8)$$

The width b of the Gaussian function has to be calibrated in separate calculations by deliberately changing the dihedral angles from their RIS values by ±10° (a value suggested by other simulations[29,30]) and monitoring the changes in the chemical shift. The deviations from the ideal dihedral value lead to variations of the chemical shift ranging from 0.2 to 2.7 ppm for different geometries. To avoid the introduction of many numerical factors, an effective width of $b = 1.5$ ppm is assumed throughout this paper for all groups and all polymers. This is certainly only a rough approximation of the "real" pattern, but it reflects the still limited present day computing power and the approximate character of the underlying statistical model. In eqs 7 and 8 the sum is over all configurations/conformations with an appreciable probability. The overall probability of the conformations considered is >90% for most of the investigated polymers. For the almost perfectly atactic poly(propylene), the configurational statistics is easily calculated $p(x_1,x_2,x_3) = (0.5)^3 = 0.125$. The experimental sample meets this distribution within experimental errors (≈2%).[18]

In the same way, the position of the configuration (x_1, x_2, x_3) in a solution spectrum is given by the averaged chemical shift

$$\sigma_K(x_1,x_2,x_3) = \sum_{j,x_1^j=x_1,x_2^j=x_2,x_3^j=x_3} p^{RIS}_{conform}(\vartheta_1^j,\vartheta_2^j,\vartheta_3^j,\vartheta_4^j|x_1,x_2,x_3)\, \sigma_K(G_j) \quad (9)$$

where the sum extends only over those geometries with the correct configuration (x_1, x_2, x_3).

The formulas for the simulation of the solid state spectrum (eq 8) and the configurational splitting (eq 9) tacitly assume that the chemical shift is an **intra**molecular effect; any **inter**molecular contribution by other polymer chains and or solvent molecules is neglected. This assertion is a *conditio sine qua non* for the validity of the method. In the case of poly(propylene) we can check it by comparing the CP/MAS spectra of two modifications of crystalline isotactic poly(propylene) (α,β-iPP); here the same *tg* helix is packed in two different ways. The chemical shifts differ by only ≈1 ppm and it may be concluded that for poly(propylene) at least and most likely for all unpolar polyolefin systems, the intermolecular contributions to the chemical shift are indeed small and may be neglected. It should be noted, however, that for polar systems and systems with hydrogen bridges, the intermolecular effect might prove to be larger.

Comparison with Experiment. When comparing experimental and theoretical data, it is essential to note that theoretical calculations yield absolute values with respect to the bare nucleus *in vacuo* whereas experimental data refer to a reference (tetramethylsilane (TMS) for ^{13}C). The experimental scale δ is related to the theoretical scale σ *via*

$$\delta = \sigma_0 - \sigma \quad (10)$$

where σ_0 is the theoretical value of the reference. In practice, the shortcomings of a still approximate quantum chemical calculation and the use of small atomic bases leads to small errors in the absolute δ-values of the various resonances (for problems of principal character see ref 6, section 3.1). But here we focus on relative effects, *i.e.* the relative shift of the resonances of the same molecule due its change in geometry, or the configurational splitting. For these questions, the error in the absolute values is not very essential (*vide infra*, section 3).

3. Results for Atactic Poly(propylene)

In this section we want to present some results on aPP to demonstrate the wealth of information that can

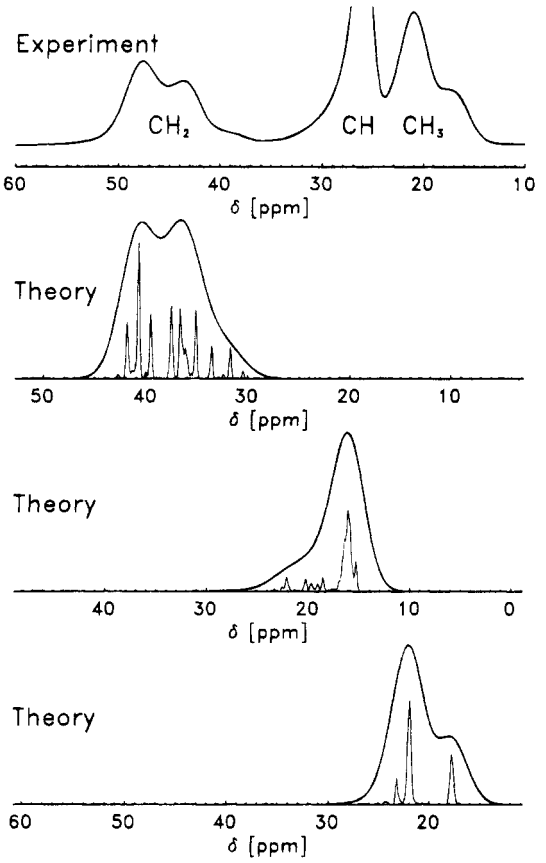

Figure 4. Experimental CP/MAS spectrum of solid glassy aPP (top) compared with simulations for the various groups (rows 2–4). For all groups the shape is satisfactorily matched. Note that for all spectra—experiment and theory—the width of the spectrum is 50 ppm. The absolute position is not correctly reproduced by the quantum chemical simulations due to the small atomic basis employed and has been adjusted for better comparison. The absolute height of the peaks does not convey any information since experimentally different cross polarization efficiencies tend to distort the stoichiometric relations. Thus, the simulated spectra were all scaled to the same peak height. The fine line shows the contributions of the various conformations, eq 7 (slightly broadened for typographical reasons); the bold line is the simulation with the δ-function being replaced by a Gaussian function, s_b, eq 8.

be obtained by the application of the method described in the previous section 2. A discussion of the configurational splitting is deferred to a special section (section 5).

Simulation and Analysis of the Solid State NMR Spectrum. The IGLO calculations were performed with an atomic basis of 2ζ-quality (DZ in the notation of ref 6) for both carbons ((7s, 3p) Huzinaga basis in (4,1,1,1;2,1) contraction) and hydrogens ((3s) in (2;1) contraction). About 90 different geometries were taken into account. The intrinsic symmetry of the model molecule was used to avoid the calculation of redundant geometries. Perfect Bernoullian configurational statistics $p_m = p_r = 0.5$ was assumed. The overall CPU time necessary for the calculation was $\approx$90·12 h = 45 days on a SGI IRIS INDIGO workstation (R4000 CPU, 64 MB RAM). We used the semidirect version of the IGLO program,[21] routinely, about 50 million integrals were stored on hard disk.

Figure 4 shows the simulation in comparison with an experimental CP/MAS spectrum of glassy aPP. The fine line displays the contributions of the various geometries (like in eq 7) which have been slightly broadened for typographical reasons. The bold line shows the overall simulation where all contributions have been convoluted with the Gaussian function s_b, eq 8. We note that the absolute heights of the resonances were adjusted arbitrarily, as the different groups have different cross polarization efficiencies. The simulated shape of the methylene unit nearly coincides with the experimental pattern. Both the two almost equally populated main contributions and the small high-field shoulder are reproduced. By investigation of the geometries contributing to these subresonances they can be assigned to conformations (ϑ_1, ϑ_2, ϑ_3, ϑ_4) = (t, *, *, t), (t, *, *, g)/(g, *, *, t), and (g, *, *, g), respectively. The conformational state of a position denoted by an asterisk (*) is not specified. This assignment confirms the empirical *γ-gauche* effect. As in the case of poly(isobutylene)[3] a further analysis shows that the naïve conception of an "exclusive" *γ-gauche* effect has to be modified, as apart from the dihedral angles other geometric parameters have an impact on the chemical shift. The methyl resonance is comparably well reproduced; the subresonances can be identified (from left to right) as (*, t, g, *)/(*, g, t, *) and (*, t, t, *) states. Note that for the methyl group, the *γ-gauche* sensitive dihedral angles are ϑ_2 and ϑ_3 rather than ϑ_1 and ϑ_4. The methine signal is narrow both in the experiment and in the simulation. In this case, however, the simulation is only indicative of a trend, since a well-defined position of both γ-neighbors of the methine carbons B_1 and B_2 requires defined values for two more dihedral angles (ϑ_0 and ϑ_5 in Figure 3) which were left undefined in the course of the present calculation.

In the fortunate case of poly(propylene) the subpeak assignment of quantum chemistry can be verified by comparison with well-defined crystalline modifications of isotactic (*tg*-helix) and syndiotactic (*ttgg*-helix) poly(propylene). Indeed, we find that our assignment exactly matches the peak identification of the crystalline samples.[1]

The overall agreement of theory and experiment puts strong evidence in favor of the statistical model employed. It must be mentioned, however, that our approach is not very sensitive to subtleties of the statistical model used. As only 90% of the conformations are taken into account and the chemical shift calculations are subject to an error of $\approx$1 ppm, deviations of that size are not significant. Moreover, experimental uncertainties (cross polarization efficiencies, proton decoupling power, homogeneity of the magnetic field) and the overall use of a single Gaussian function in eq 8 tend to obscure fine details. Nevertheless, the compatibility of experiment and simulation can be established. In this sense, the five-state RIS model[10] for aPP seems to be valid in the glassy state even on a strictly local length scale.

Influence of the Atomic Basis on the Calculated Values of the Chemical Shift. As already mentioned in section 2 and clearly evidenced in Figure 4, the absolute positions of the various groups do not coincide with the experimental values, whereas the range and the shape are well reproduced. This defect is largely due to the small size of the atomic basis used in the IGLO calculation. To assess this effect, a small number of selected geometries were also calculated with a larger atomic basis of 3ζ-quality (II′ in the notation of ref 6: (9s, 5p, 1d) contracted to (5,1,1,1,1;2,1,1,1;1) for carbons, (3s) in (2,1) contraction for hydrogens). In Figure 5, the chemical shifts obtained with this larger basis are plotted *vs* the DZ shifts (see Simulation and Analysis of the Solid State NMR Spectrum, section 3). For all the structural elements of aPP, there is an excellent linear correlation with unity slope. The ordinate shift,

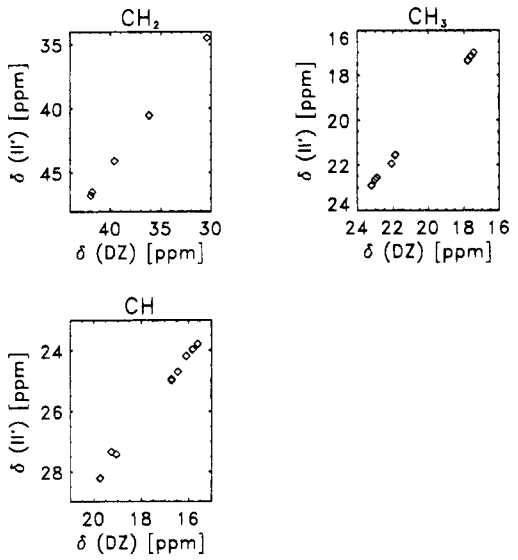

Figure 5. Chemical shift obtained with the medium-sized 3ζ-basis II′ plotted against the DZ chemical shifts for the various groups and for a few selected geometries of aPP. We find an excellent linear correlation with unity slope. The ordinate shifts, however, are non-zero and depend on the chemical group. This shows that the small basis DZ does not yield correct absolute shifts. Relative shifts are adequately calculated even with the small atomic basis.

however, is different for each group. This finding indicates that the absolute values of the chemical shifts are not propery evaluated with a small atomic basis whereas the relative geometry-induced shifts are in excellent agreement with large basis results. Thus, for our purposes, the small atomic basis is sufficient. This assertion would not hold if we intended to calculate the solution spectrum of a newly synthesized molecule. In this case, it is the absolute shift that matters and at least 3ζ-precision is required. If we use the ordinate shifts of Figure 5 as a correction for the simulation (Figure 4), the errors in the absolute shifts are considerably reduced and do not exceed 2.5 ppm. With an even larger basis for the calibration (in place of II′), the errors are expected to be even smaller.

Molecular Orbital Contribution to the Chemical Shift. The IGLO method permits the identification of localized molecular orbital contributions to the chemical shift. An analysis shows that the chemical shift is indeed a very local phenomenon. The most important orbitals for a methylene carbon are the carbon 1s orbital and the four adjacent σ-bonds (two C−C bonds and two C−H bonds). The four bonds depend on the geometry whereas the core 1s electron of the carbon itself is virtually geometry independent. Each of the other remote molecular orbitals contributes less than 1 ppm; their total sum is ≈3.5 ppm and is not sensitive to geometry variations. The strictly local character of the chemical shift is essential for the method described in this paper. If remote orbitals contributed significantly, the cutting of long molecules and the usage of small model molecules for quantum chemistry calculations would not be appropriate or justified.

Anisotropy of the Chemical Shift. As mentioned in section 2, the chemical shift is a tensorial quantity; *i.e.* it is anisotropic and depends on the orientation of the molecule with respect to the magnetic field. In a static 1D NMR experiment of a simple, well-defined polycrystalline "powder" sample, typical powder patterns are recorded (Figure 6), the singularities being interpreted as the principal components σ_{xx}, σ_{yy}, and σ_{zz} of the diagonalized shift tensor. In systems with

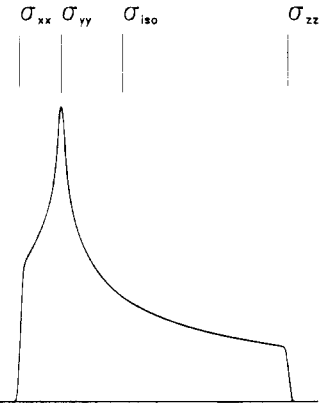

Figure 6. Typical powder pattern reflecting the anisotropy of the chemical shift. The edges of the pattern and the maximum give the principal tensor components σ_{xx}, σ_{yy}, and σ_{zz} directly. In complicated disordered systems, different powder patterns overlap and the resulting spectrum is usually too complicated for an interpretation.

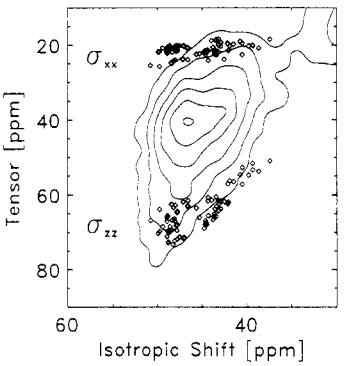

Figure 7. Isotropic−anisotropic separation spectrum of the methylene region of glassy atactic poly(propylene) recorded at $T \approx 240$ K on a Bruker MSL-300 with a DAS probe head. The two angles for evolution and detection, respectively, were $\vartheta_1 = 81.7°$ and $\vartheta_2 = \vartheta_m = 54.7°$. The rotation frequency was 3000 Hz, and 128 t_1 increments were recorded. The theoretical values (◇) are superimposed on the experimental contour plot. The absolute positions were adjusted like in the 1D spectrum. A qualitative agreement of theory and experiment is seen.

multiple resonances or inhomogeneous broadening, the different powder patterns usually overlap and yield a complicated spectral distribution, which conveys little information. The experimental investigation of the anisotropy of the chemical shift in disordered solid samples therefore often requires special experimental techniques. The separation of the anisotropy patterns for different isotropic chemical shifts is of special interest and can be obtained in a 2D **D**ynamic **A**ngle **S**pinning (DAS) experiment (see ref 31, Chapter 6.4/6.5).[32-34] In this conceptually simple but experimentally demanding approach, the angle of the rotation axis with the external magnetic field is different in the evolution and detection period, respectively; for further details we refer to the literature. The contour plot in Figure 7 shows a preliminary isotropic/anisotropic separation spectrum of the methylene unit. For every isotropic shift on the x-axis, the intensity distribution along the y-axis displays the corresponding powder pattern; the edges correspond to σ_{xx} and σ_{zz}, as indicated in the figure. Sine the IGLO method delivers the full tensor and not just the isotropic value, the experimental findings can now be compared with the theoretical predictions. The theoretical values of the xx- and the zz-components are superimposed on the experimental contour plot in Figure 7 and symbolized by the little diamonds (◇). The absolute values were adjusted in the

same way as for the isotropic chemical shift. The spectral position of σ_{yy} is not easily seen in the experimental spectrum; to keep the figure simple, the theoretical values for σ_{yy} have been omitted.

We find that σ_{xx} does not vary much with the isotropic shift whereas the variation of σ_{zz} is considerably larger ($\approx$20 ppm) and dominates the variations of the isotropic chemical shift. The same trend is observed in the experimental spectrum. As a consequence, the size of the anisotropy $[\sigma_{xx} - \sigma_{zz}]$ decreases with decreasing isotropic shift in both the simulation and the experiment. Thus, in addition to the isotropic chemical shift, the anisotropic part of the shift tensor might be used as a source of structural information.

4. Other Systems

The polymers that have been inquired with a similiar method are listed in Table 1. Additional information on the statistical model employed is also included; the model molecules are listed in Figure 1. In this section we present some selected results. A more detailed account with additional figures which here have been omitted for reasons of limited space will be published in a forthcoming review.[8] All compounds (including aPP) were used as purchased or obtained from synthesis. If the glass transition temperature T_g of the sample was below room temperature, the glassy state was reached by cooling the sample in a stream of cool air in the course of the MAS measurement. No special procedures (like precipitation from solution) were chosen to influence the microstructure of the glassy state. If technically possible, the samples were heated above T_g and cooled again in the course of the NMR measurements. In neither case were appreciable deviations in the amorphous spectrum observed. (For PE, the degree of crystallinity changed upon heating and cooling, but the shape of the amorphous spectrum was unchanged.)

Poly(ethylene). Poly(ethylene) (PE) is the simplest polymer and permits the investigation of fundamental questions. The ^{13}CCP/MAS spectrum of amorphous glassy PE is very simple and consists of a single Gaussian peak, which is satisfactorily reproduced by the simulation. (For more information about the still debated question of the glass transition in PE see, *e.g.*, ref 35.) More interestingly, the chemical shift displays a pronounced geometry dependence. In Figure 8b the chemical shift of the central atom (A) is plotted versus the added moduli of the dihedral angles that are relevant for the position of the γ-neighbors, $|\vartheta_1| + |\vartheta_4|$. A correlation of the chemical shift with $|\vartheta_1| + |\vartheta_4|$ is observed; in this respect, the *γ-gauche* effect is confirmed. On the other hand, even for fixed $|\vartheta_1| + |\vartheta_4|$ we see a considerable spread in the chemical shifts. Thus we may conclude that the chemical shift does not depend exclusively on these dihedral angles but also on other geometric parameters. In the simple case of PE these paramters can be identified. In Figure 8c the chemical shift is plotted versus the mean distances of the carbon γ-neighbors. The observed correlation is another manifestation of the *γ-gauche* effect. But again, for fixed distances, the chemical shift is spread over $\approx$6 ppm. The *γ-gauche* effect is thus not a simple steric phenomenon; the distance of the γ-neighbors is important but not decisive. In Figure 8d only the chemical shifts of the geometries with $|\vartheta_1| + |\vartheta_4| \approx 115°$ (*i.e.* $(\vartheta_1, \vartheta_2, \vartheta_3, \vartheta_4) = (t, *, *, g)$ or $(g, *, *, t)$) are displayed against $|\vartheta_2| + |\vartheta_3|$. An excellent correlation with very little residual unexplained jitter is observed. For the other clusters with $|\vartheta_1| + |\vartheta_4| \approx 0°, 230°$, the same pattern emerges. Thus,

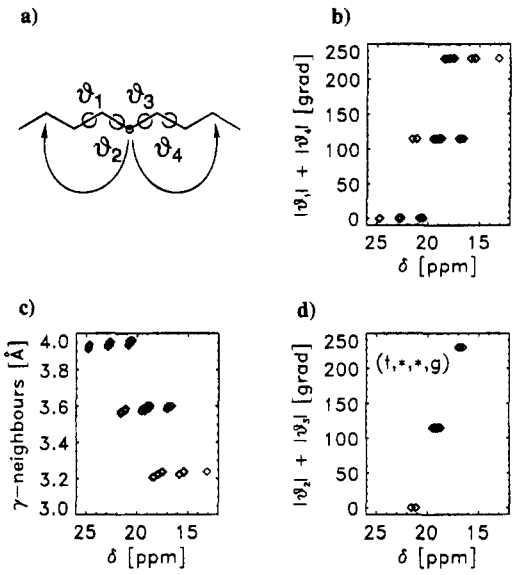

Figure 8. Geometrical parameters which are important for the chemical shift of the central methylene atom in PE (a). The *γ-gauche* effect is essentially confirmed (b, dihedral angles *vs* chemical shift) and is shown to be of partially steric origin (c, mean γ-distances *vs* chemical shift). For each of the clusters of fixed $|\vartheta_1| + |\vartheta_4|$ in (b) the observed spread in the chemical shift can be correlated with $|\vartheta_2| + |\vartheta_3|$, as exemplified for one cluster (d). For PE, the geometrical origin for the non-*γ-gauche* contribution to the chemical shift is thus identified.

the interior dihedral angles ϑ_2 and ϑ_3 are almost as important as the exterior "*γ-gauche*-dihedrals" ϑ_1 and ϑ_4. The naïve phenomenological conception of a *γ-gauche* effect depending exclusively on the *trans/gauche* character of the ϑ_1, ϑ_4-bonds has to be modified. For studies of solution NMR spectra (*vide infra*, section 5), this *ansatz* might suffice, especially if one has the freedom to adjust phenomenological parameters (like *γ-gauche* constants), but for more detailed investigations a refined view of the *γ-gauche* effect is necessary.

In all the other systems investigated, the spread of the chemical shift for fixed *γ-gauche* dihedral angles (like in Figure 8b) is observed, too. Due to their more complicated geometry, the source of this spread is not as easily identified as in the case of PE, but the essential feature still holds: It is not only the "traditional" dihedral angles that have an impact on the chemical shift.

Poly(isobutylene). Poly(isobutylene) (PIB) is a bisubstituted polyolefin with a very "crowded" structure. The CP/MAS spectrum of glassy PIB displays very broad and partially structured resonances whose principal features are well reproduced by the simulation. As in the case of PE and aPP, the *γ-gauche* effect is essentially confirmed; again the observed spread for fixed *γ-gauche* dihedral angles must be attributed to the influence of other geometric parameters. Moreover a nice correlation of the chemical shift with the length of the adjacent carbon–carbon bonds has been observed. A more detailed account of the results has already been published.[3]

1,4-Poly(butadiene) and 1,4-Poly(isoprene). Poly(butadiene) (PBD) and poly(isoprene) (PIP) are unsaturated polymers and were chosen to investigate the influence of double bonds on the degree of agreement between experiment and theoretical results. In systems with double bonds, correlation effects might take place that require a beyond-Hartree–Fock treatment which is not implemented in the current version of IGLO. Indeed, the results are less convincing than in the other

Table 3. *Cis-Trans* Splitting (ppm) for 1,4-Poly(butadiene)

typ	exp[36] 333 K	IGLO (DZ) 330 K	IGLO (II') 330 K
CH_2	5.2	5.7	6.3
CH=	0.6	2.9	3.6

Table 4. *Cis–Trans* Splitting (ppm) $\Delta\delta = \delta_{cis} - \delta_{trans}$ for the Different Positions in 1,4-Poly(isoprene)

position	exp[36] 298 K	IGLO (DZ) 300 K	IGLO (II') 300 K
A	not resolved	0.2	0.5
B	7.6	7.7	8.9
C	not resolved	0.6	1.5
D	0.9	1.7	2.5
E	7.6	4.4	4.1

systems. Tables 3 and 4 show the calculated *cis–trans* splittings for the various positions in comparison with experimental data.[36] Especially the calculated chemical shifts of the methyl position of PIP deviate significantly from experiment. On the other hand, some features of the experimental solid state spectrum are nicely met. The partial failure of the method in these systems requires additional research, as the reasons are quite unclear. Apart from correlation effects (which would call for improvements on the quantum chemistry side), shortcomings of the empirical force field (which would call for a better parametrization) might be responsible for the problems.

Poly(vinyl chloride). Poly(vinyl chloride) (PVC) is a monosubstituted vinyl polymer that contains chlorine as a heteroatom and was chosen for this reason as a challenging system to investigate the capabilities of the method. The presence of the heteroatom does not deteriorate the applicability of the method. We find a satisfactory agreement between the simulated and experimental solid state spectrum ($(mm) = 17\%$, $(mr) = 51\%$, $(rr) = 32\%$). A quite pronounced *γ-gauche* effect is observed. Calculations with a larger atomic basis (II') reveal that even in this case the small basis DZ is sufficient to obtain reliable results. We may conclude that heteroatoms are not an *a priori* obstacle to the application of the method.

Poly(methyl methacrylate). Poly(methyl methacrylate) (PMMA) is a vinyl polymer with two side groups, one of which is extended ($COOCH_3$) and has internal degrees of freedom. This fact is a considerable nuisance for the simulation as the number of relevant geometries is multiplied, and the necessary computing power increases substantially. PMMA is a special case, as both the appropriate RIS model and the molecular organization in the amorphous solid state are still a matter of controversy.[37] Whereas the random coil model is confirmed by neutron scattering data on a larger length scale, both recent NMR investigations[38–40] and X-ray experiments[41–43] indicate some local order in the solid state and a deviation from a completely random organization on a local length scale. This should show up in the ^{13}C solid state NMR spectrum, too. Indeed, we find only a very poor agreement between the experimental spectrum and the simulation, which is based on the six-state RIS model[17] and thus implicitly the random coil assumption (Figure 9 shows the case of the methyl unit as an example; for the experimental stereostatistics, see the figure caption). Generally, the experimental resonances are narrower than those in the simulation. One explanation for this finding is that the molecular organization of PMMA might be truly a special case and present some degree of order not

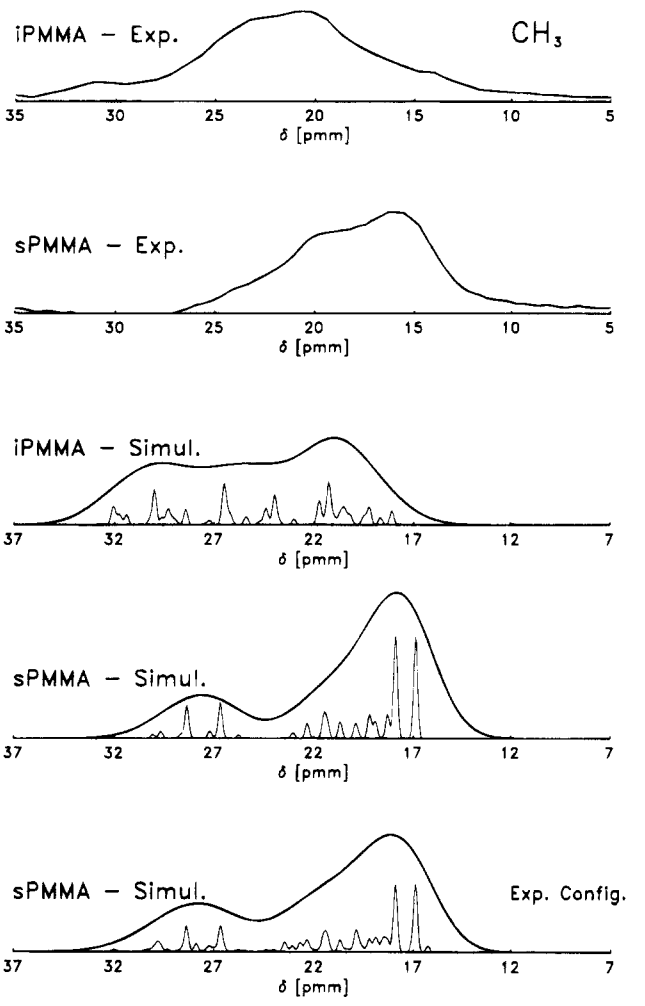

Figure 9. Top to bottom: experimental spectrum of almost ideally isotactic PMMA ($(mm) > 95\%$), experimental spectrum of preferentially syndiotactic PMMA ($(rr) = 62\%$, $(mr) = 30\%$, $(mm) = 8\%$), simulation for ideally isotactic PMMA, simulation for ideally syndiotactic PMMA, simulation of PMMA with the configurational statistics of the experimental preferentially syndiotactic sample. Only the methyl region of the spectra is shown. Compared with aPP (Figure 4), the agreement between experiment and theory is poor. Especially for the syndiotactic sample, the simulated line shape is broader than the experimental one, which is indicative of some residual order in the amorphous glassy state. The spectra of the other groups (C_α, COO) not shown here display a similar behavior. As in Figure 4, the fine lines show the contributions of the various conformations and the bold lines, the overall simulation with the Gaussian broadening function s_b.

accounted for in the statistical model. Other reasons, however, are not yet excluded. The RIS model employed might be generally defective (but see the successful prediction of the configurational splitting, section 5); the force field parametrization could be inappropriate; *etc.*

Apart from this unresolved question, one finding is especially interesting. In Figure 10b the methyl carbon shift is plotted *vs* $|\vartheta_2| + |\vartheta_3|$, the sum of the moduli of the dihedral angles that should determine the position of the γ-neighbors. No *γ-gauche* effect is apparent; *i.e.* the *trans/gauche* character of the bonds described by ϑ_2 and ϑ_3 is not decisive for the chemical shift. The pattern is more complicated. In Figure 10c a correlation of the methyl chemical shift with the mean distance of the γ-neighbors is clearly discernible although the considerable spread reveals nonsteric factors. The reason for this seemingly paradox situation—no obvious dependence on the dihedral angles, but appreciable correlation with the γ-distances—is given in Figure 10d: The

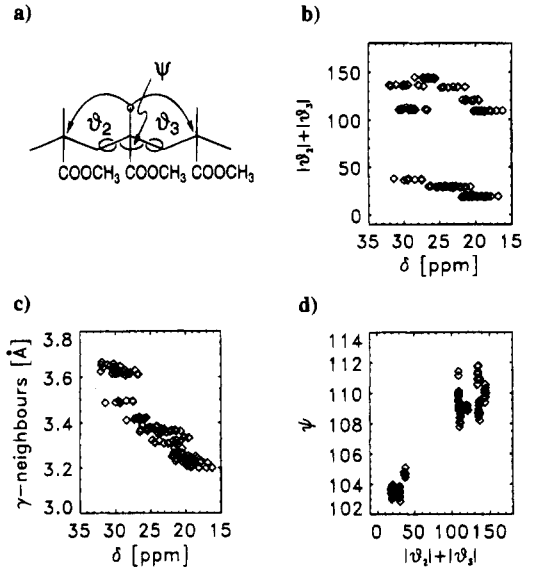

Figure 10. Geometrical situation in PMMA (a). The chemical shift of the central methyl unit is not correlated with the dihedral angles $|\vartheta_2| + |\vartheta_3|$ (b), but astonishingly with the mean distance of the main chain γ-neighbors (c). In PMMA, the central bond angle ψ widens considerably, if the adjacent bonds are in a *gauche* state (d). Thus, the dihedral angles are no longer a good indicator of the geometrical situation.

central **bond** angle ψ (see Figure 10a) changes with $|\vartheta_2| + |\vartheta_3|$. The phenomenological model of the *γ-gauche* effect assumes a strictly tetrahedral coordination; then the γ-distances depend on the value of the respective dihedral angle alone. In all systems investigated, this assumption holds only approximately, but in PMMA the assertion even completely fails. The dihedral angles are no longer a good indicator of the geometric situation. Consequently, the empirical rules to predict the configurational splitting which rely on the simple model of tetrahedral coordination are bound to fail.[2] We will discuss this point in more detail in section 5.

5. Configurational Splitting

Vinyl polymers with one substituent or two different substituents have pseudoasymmetric centers and their solution spectra display a **configurational** splitting. The different conformational states (*trans*, *gauche*, ...) are averaged on the NMR time scale by rapid conformational transitions, whereas the activation energy for a configurational transition in the absence of a catalyst is much higher than the thermal energies. Consequently, configurational transitions do not take place, and configurational averaging, *e.g.* between an *m* and an *r* diad, is not observed. The various peaks belonging to the same group are thus conformationally averaged, but not configurationally.

This configurational splitting can be calculated by the combination of a statistical model and *ab initio* IGLO chemical shift calculations, as shown in eq 9, which is here repeated for the special case of the central methylene unit A (Figures 1 and 3) of poly(propylene).

$$\sigma_A(x_1,x_2,x_3) = \sum_{j,x_1^j=x_1,x_2^j=x_2,x_3^j=x_3} \underbrace{p^{RIS}_{conform}(\vartheta_1^j,\vartheta_2^j,\vartheta_3^j,\vartheta_4^j|x_1,x_2,x_3)}_{\text{statistics}}\ \underbrace{\sigma_A(G_j)}_{\text{IGLO}} \quad (11)$$

This formula (itself a simplification) can be further simplified to obtain an expression that does not rely any longer on the time consuming quantum chemical calculations. We adopt a simple two-state model (*t*, *g*) for the time being and assume that σ_{CH_2} depends only on ϑ_1^j and ϑ_4^j. Additionally, we state that σ_{CH_2} consists of a constant absolute value σ_{abs} depending on the chemical bonding situation and a geometry-depending contribution γ_{CH_2}, that is effective only if either ϑ_1 or ϑ_4 is in a *gauche* state.

$$\sigma_A(G^j) = \sigma_{abs} + \gamma_{CH_2}\delta_{\vartheta_{1_g}} + \gamma_{CH_2}\delta_{\vartheta_{4_g}} \quad (12)$$

Then, eq 11 is simplified and transforms into

$$\sigma_A(x_1,x_2,x_3) = \sigma_{abs} + \gamma_{CH_2} P_{gauche,\vartheta_1}(x_1,x_2,x_3) + \gamma_{CH_2} P_{gauche,\vartheta_4}(x_1,x_2,x_3) \quad (13)$$

where $P_{gauche,\vartheta_i}(x_1,x_2,x_3)$ is the probability that ϑ_i is in a *gauche* state. γ_{CH_2} is now an empirical constant that has to be adjusted by comparison with experiment. The absolute value σ_{abs} is not important in applications as only the splitting (*e.g.* $\sigma(mmm) - \sigma(rrr)$) matters and σ_{abs} cancels. The probability P_{gauche,ϑ_i} depends on the configuration (x_1, x_2, x_3) or even larger configurational sequences (x_0, x_1, x_2, x_3, x_4, x_5), *etc.* The experimentally evidenced influence of long configurational sequences is not at variance with the strictly local character of the chemical shift, as a remote asymmetric carbon atom acts by changing the probability rather than the *γ-gauche* constant γ_{CH_2}.

The formula eq 13 is the essence of the empirical *γ-gauche* method advocated mainly by Tonelli and coworkers.[1] It has been applied with considerable success to the interpretation of solution spectra of various vinyl polymers. By introducing more *γ-gauche* constants, one can adapt it to multiple state RIS models.

For simple systems, eq 12 still conveys some truth, and the configurational splitting calculated by the more exact quantum chemistry formula eq 11 and the empirical expression eq 13 should yield comparable results. This is demonstrated by the configurational splitting of the methylene unit in aPP (Figure 11). The theoretical values are plotted against the experimental results. For both methods, the correlation is quite good, though the established empirical method seems to be somewhat better. When the results are compared, two points must be recalled.

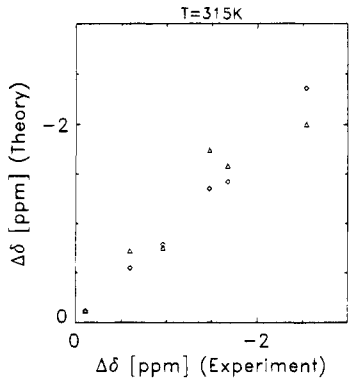

Figure 11. Configurational splitting for the methylene position in poly(propylene) at T = 315 K. The predictions of the IGLO calculations (△) and the empirical *γ-gauche* method (◇) are plotted *vs* experimental results. The experimental results and the empirical predictions were taken from ref 44, where hexad assignments (x_0, x_1, x_2, x_3, x_4) are given. For a better comparison with the IGLO results (tetrad resolution) an average over the exterior diads x_0 and x_4 has been performed.

Table 5. Configurational Splitting of the Tertiary Carbon in Poly(vinyl chloride)[a]

diad	exp[45]	exp[36]	IGLO (DZ)	emp method[45]
mm	0.0	0.0	0.0	0.0
mr	0.85	1.0	0.73	0.85
rr	1.65	1.9	1.97	1.55

[a] The value for the *mm* diad has been set to 0 ppm. The experimental values have been determined graphically from ref 45 with an accuracy of ≈0.1−0.2 ppm.

1. In the quantum chemistry calculations only the most important geometries can be taken into account; at $T = 315$ K their overall probability does not exceed 85%; the missing probability is dispersed over many hundred geometries and is naturally a source of uncertainty. On the other hand, the empirical method is not limited by computer time considerations and always treats all geometries.

2. The empirical method has the freedom to choose (within certain limits) the values of the *γ-gauche* constants. Such an adjustment naturally improves the correlation. The quantum chemistry method does not have a free parameter.

In the case of PVC, both methods fail in predicting the methylene splitting as in this case solvent effects dominate, which are not taken into account.[45] For the tertiary carbons both approaches yield comparable results (Table 5).

For PMMA, the situation is different. As we have seen in section 4, there is no evidence for a simple *γ-gauche* effect (Figure 10b) that could be approximately parametrized by a formula comparable to eq 12. Consequently, the empirical method should fail, which was indeed reported.[2] On the other hand, the quantum chemistry approach does not rely on special assumptions. In Figure 12 the simulation results for the three investigated groups (C_α, CH_3, COO) are compared with experimental data taken from ref 36. Note that neither the empirical method nor the quantum chemistry approach provide absolute values for the chemical shift, but only splittings. We find a very good correlation between calculated and experimental values for the configurational splitting.

In this special case, quantum chemistry could resolve a puzzle that is caused by the unusual geometry dependence of the chemical shift. For other systems with a well-behaved chemical shift, quantum chemistry is to be considered as a theoretical justification of the empirical method, which is superior in practical applications because it needs few computer resources and takes into account all geometries and not just the important ones. In addition, the empirical method is so far superior in resolving finer details (hexad assignments). Both methods rely on a predominantly intramolecular origin of the chemical shift, solvent effects being still untractable.

6. Conclusion and Outlook

In this study we present a new method for the analysis of both inhomogeneously broadened solid state NMR spectra of amorphous glassy polymers and the configurational splitting of vinyl polymers in solution. The method combines conformational statistics (in our case taken from the literature) and *ab initio* IGLO calculations. The method is applicable to polymer systems of different structural classes, including unsubstituted, monosubstituted, and bisubstituted polyolefins (PE, aPP, PIB), systems with heteroatoms (PVC) and extended side groups (PMMA), and even (to a certain degree) unsaturated polymers (PBD, PIP). For most systems we find a remarkable agreement between experiment and theory.

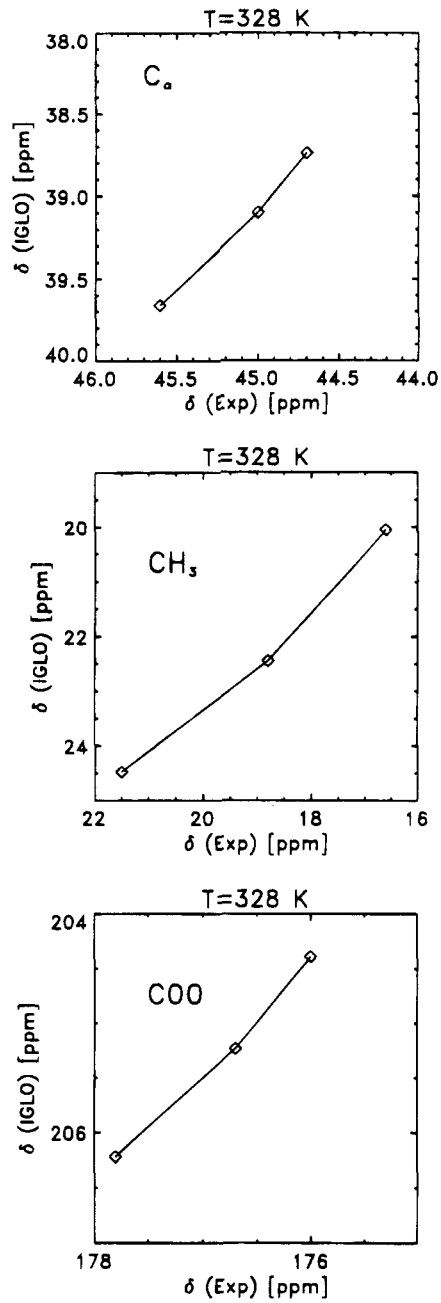

Figure 12. Configurational splitting for C_α, CH_3, and COO carbons, as predicted by IGLO, in excellent agreement with experimental data, taken from ref 36.

Furthermore, a variety of information can be obtained by the analysis of the theoretical data. The observed spread in the ^{13}C chemical shift is shown to be of predominantly conformational origin. For most systems, the empirical *γ-gauche* rules provide a reasonable qualitative description. For more detailed information, however, *ab initio* investigations are necessary. This is strikingly seen in the case of PMMA which exhibits an unusual dependence of the chemical shift on the dihedral angles. In the simple case of PE, the non-*γ-gauche* contribution to the chemical shift is identified; the interior dihedral angles are shown to have a considerable impact. By an MO analysis, it is demonstrated that the chemical shift is a strictly local phenomenon. Additional calculations with extended atomic basis sets show that for **relative** geometry-depending

effects, even modest basis sets of 2ζ-quality are sufficient. An exploratory study suggests that in addition to the isotropic chemical shift the anisotropy may be used as a source of structural information. In the near future, the steady increase in computing power will permit the investigation of more subtle problems. The modular character of our approach allows the replacement of certain components by more refined approaches, including novel statistical models, better geometry optimization (by third generation empirical force fields or SCF-MP), and advanced chemical shift calculation schemes (*e.g.* MC-IGLO,[46,47] GIAO-MBPT[48,49]). Further investigations along these lines should resolve open questions like the unknown reason for the problems in unsaturated systems.

The advent of high-resolution multiple quantum solid state NMR spectroscopy[50-53] should make it possible to eventually probe the geometrical parameters discussed here directly and relate it to the chemical shift. Thus, the combination of experimental NMR and theoretical studies provides a way to have a thorough look on the **local** organization of disordered polymeric systems which is a useful complement of the scattering methods which elucidate mainly larger length scales.

Acknowledgment. The authors thank Prof. Dr. W. Kutzelnigg, Dr. M. Schindler, und Dr. U. Fleischer for providing the IGLO program and for useful discussions.

References and Notes

(1) Tonelli, A. E. *NMR* Spectroscopy *and Polymer Microstructure: The Conformational Connection*; VCH: Weinheim, New York, 1989.
(2) Tonelli, A. E. *Macromolecules* **1991**, *24*, 3065–3068.
(3) Born, R.; Spiess, H. W.; Kutzelnigg, W.; Fleischer, U.; Schindler, M. *Macromolecules* **1994**, *27*, 1500–1504.
(4) Kutzelnigg, W. *Isr. J. Chem.* **1980**, *19*, 193–200.
(5) Kutzelnigg, W. *THEOCHEM* **1989**, *202*, 11–61.
(6) Kutzelnigg, W.; Fleischer, U.; Schindler, M. *NMR Basic Princ. Prog.* **1991**, *23*, 165–262.
(7) Flory, P. J. *Statistical Mechanics of Chain Molecules*; Interscience Publishers: New York, 1969.
(8) Born, R.; Spiess, H. W. *NMR Basis Princ. Prog.*, in press.
(9) Raucchi, R.; Vacatello, M. *Makromol. Chem., Theory Simul.* **1993**, *2*, 875–888.
(10) Suter, U. W.; Flory, P. J. *Macromolecules* **1975**, *8*, 765–776.
(11) Vacatello, M.; Yoon, D. Y. *Macromolecules* **1992**, *25*, 2502–2508.
(12) Abe, Y.; Flory, P. J. *Macromolecules* **1971**, *4*, 219–229.
(13) Abe, Y.; Flory, P. J. *Macromolecules* **1971**, *4*, 230–238.
(14) Williams, A. D.; Flory, P. J. *J. Am. Chem. Soc.* **1969**, *91*, 3111–3118.
(15) Williams, A. D.; Flory, P. J. *J. Am. Chem. Soc.* **1969**, *91*, 3118–3121.
(16) Mark, J. E. *J. Chem. Phys.* **1972**, *56*, 451–458.
(17) Vacatello, M.; Flory, P. J. *Macromolecules* **1986**, *19*, 405–415.
(18) Zemke, K. Untersuchungen zur Konformation und Dynamik von amorphen Polymeren mit mehrdimensionaler Festkörper-^{13}C-NMR. Ph.D. thesis, Johannes Gutenberg Universität, Mainz, 1994.
(19) Zemke, K.; Schmidt-Rohr, K.; Spiess, H. W. *Acta Polym.* **1994**, *45*, 148–159.
(20) Kirste, R. G.; Kruse, W. A.; Ibel, K. *Polymer* **1975**, *16*, 120–124.
(21) Meier, U.; Wüllen, Ch. van; Schindler, M. *J. Comput. Chem.* **1992**, *13*, 551–559.
(22) Hameka, H. *Mol. Phys.* **1958**, *1*, 203–215.
(23) Pople, J. A. *J. Chem. Phys.* **1962**, *37*, 53–59.
(24) Ditchfield, R. *J. Chem. Phys.* **1972**, *56*, 5688–5691.
(25) Wolinski, K.; Hinton, J. F.; Pulay, P. J. *J. Am. Chem. Soc.* **1990**, *112*, 8251–8260.
(26) Hansen, A. E.; Bowman, T. D. *J. Chem. Phys.* **1985**, *82*, 5035–5047.
(27) Hansen, A. E.; Bouman, T. D. Ab-initio calculation and analysis of nuclear magnetic shielding tensors: the LORG and SOLO approaches. In *Nuclear Magnetic Shielding and Molecular Structure*; Tossel, J. A., Ed.; NATO ASI Series; Kluwer Academic Publishers: Dordrecht, Boston, London, 1993; pp 95–116.
(28) Biosym, Inc. DISCOVER, 1993.
(29) Theodorou, D. N.; Suter, U. W. *Macromolecules* **1985**, *18*, 1467–1478.
(30) Mansfield, K. F.; Theodorou, D. N. *Macromolecules* **1991**, *24*, 6283–6294.
(31) Schmidt-Rohr, K.; Spiess, H. W. *Multidimensional Solid State NMR and Polymers*; Academic Press: New York, 1994.
(32) Bax, A.; Szeverenyi, N. M.; Maciel, G. E. *J. Magn. Reson.* **1983**, *55*, 494–497.
(33) Maciel, G. E.; Sveverenyi, N. M.; Sardashti, M. *J. Magn. Reson.* **1985**, *64*, 365–374.
(34) Terao, T.; Fujii, T.; Onodera, T.; Saika, A. *Chem. Phys. Lett.* **1984**, *107*, 145–148.
(35) van Krevelen, D. W.; Hoftyzer, P. J. *Properties of Polymers*; Elsevier: Amsterdam, 1976.
(36) Pham, Q. T.; Petiard, R.; Waton, H.; Llauro-Darricades, Marie-France. *Proton and Carbon NMR Spectra of Polymers*; Penton Press: London, 1991.
(37) Vacatello, M.; Yoon, D. Y.; Flory, P. J. *Macromolecules* **1990**, *23*, 1993–1999.
(38) Kulik, A. S.; Beckham, H. W.; Schmidt-Rohr, K.; Radloff, D.; Pawelzik, U.; Boeffel, C.; Spiess, H. W. *Macromolecules* **1994**, *37*, 4746–4754.
(39) Kulik, A. S.; Radloff, D.; Spiess, H. W. *Macromolecules* **1994**, *27*, 3111–3113.
(40) Kulik, A. S.; Spiess, H. W. *Macromol. Chem. Phys.* **1994**, *195*, 1755–1762.
(41) Miller, R. L.; Boyer, R. F. *J. Polym. Sci., Polym. Phys. Ed.* **1984**, *22*, 2021–2041.
(42) Miller, R. L.; Boyer, R. F. *J. Polym. Sci. Polym. Phys. Ed.* **1984**, *22*, 2043–2050.
(43) Windle, A. H. *Measurements of Molecular Orientation and Structure in Non-Crystalline Polymers with Wide Angle X-Ray Diffraction*; Ward, I. M., Ed.; Developments in Oriented Polymers Applied Science *Publishers*: London, New York, 1982; Vol. 1, pp 1–46.
(44) Schilling, F. C.; Tonelli, A. E. *Macromolecules* **1980**, *13*, 270–275.
(45) Tonelli, A. E.; Schilling, F. C.; Starnes, Jr.; W. H.; Shepherd, L.; Plitz, I. M. *Macromolecules* **1979**, *12*, 78–83.
(46) Kutzelnigg, W.; van Wüllen, Ch.; Fleischer, U.; Franke, R.; von Mourik, T. The IGLO method. Recent developments. In *Nuclear Magnetic Shielding and Molecular Structure*; NATO ASI Series; Kluwer Academic Publishers; Dordrecht, Boston, London, 1993; pp 141–162.
(47) van Wüllen, Ch.; Kutzelnigg, W. *Chem. Phys. Lett.* **1993**, *205*, 563–571.
(48) Gauss, J. *J. Chem. Phys.* **1993**, *99*, 3629–3642.
(49) Gauss, J. *Chem. Phys. Lett.* **1994**, *229*, 198–203.
(50) Geen, H.; Titman, J. T.; Gottwald, J.; Spiess, H. W. *Chem. Phys. Lett.* **1994**, *227*, 79–86.
(51) Sommer, W.; Gottwald, J.; Demco, D. E.; Spiess, H. W. *J. Magn. Reson.* **1995**, *A113*, 131–134.
(52) Geen, H.; Titman, J. J.; Gottwald, J.; Spiess, H. W. *J. Magn. Reson.* **1995**, *A114*, 264–267.
(53) Gottwald, J.; Demco, D. E.; Graf, R.; Spiess, H. W. *Chem. Phys. Lett.* **1995**, *243*, 314–323.

MA950975H